PHYSICAL REVIEW B VOLUME 32, NUMBER 12 15 DECEMBER 1985

Calculation of the surface segregation of Ni-Cu alloys with the use of the embedded-atom method

S. M. Foiles
Sandia National Laboratories, Livermore, California 94550

(Received 5 August 1985)

The surface composition of Ni-Cu alloys has been calculated as a function of atomic layer, crystal face, and bulk composition at a temperature of 800 K. The results show that the composition varies nonmonotonically near the surface with the surface layer strongly enriched in Cu while the near-surface layers are enriched in Ni. The calculations use the embedded-atom method [M. S. Daw and M. I. Baskes, Phys. Rev. B **29**, 6443 (1984)] in conjunction with Monte Carlo computer simulations. The embedding functions and pair interactions needed to describe Ni-Cu alloys are developed and applied to the calculation of bulk energies, lattice constants, and short-range order. The heats of segregation are computed for the dilute limit, and the composition profile is obtained for the (100), (110), and (111) surfaces for a variety of bulk compositions. The results are found to be in accord with experimental data.

I. INTRODUCTION

A detailed knowledge of the structure of alloy surfaces is important for the understanding of many surface phenomena such as corrosion and catalysis. However, the surface composition and structure can be very different from that in the bulk; for example, Cu is enriched in the surface layer of Ni-Cu alloys as will be discussed below. In applications such as catalysis, it is the surface composition that is important. In particular, the chemical reactivity of catalysts can be tailored to enhance the production of the desired products by the suitable choice of binary alloys. This represents the variation in the relative abundance of different configurations of the metallic species on the surface. By varying the relative number of different types of adsorption sites, the relative rates of the chemical reactions catalyzed by these configurations can be adjusted. Thus it is important to know both the overall composition of the surface as well as the compositional order, if any, in the surface layer. The latter affects the availability of different atomic configurations of alloy species on the surface. The goal of this work is to apply the recently developed embedded-atom method (EAM) to the determination of the composition and structure of alloy surfaces.

There have been numerous theoretical efforts to determine the surface composition of alloys from a knowledge of the bulk thermodynamics.[1-5] The most common microscopic approach is the lattice-gas model[6,7] (also known as the bond-breaking model). The atoms are assumed to sit on ideal lattice sites and interact with their nearest neighbors only. The interaction energies between atoms of the same species are chosen to give the correct heats of sublimation of the bulk alloys. The interactions between the different species are either taken to be the average of the pure metal interactions (ideal solution) or adjusted to approximately reproduce the variation of the enthalpy of the bulk alloys with composition (regular solution). However, this approximation for the energetics has several deficiencies. First, the interactions in real metals are longer ranged than first neighbors only. Also, the bond energies for atoms on the surface need not be the same as in the bulk due to the difference in the local environment of the surface atoms. In fact, some models attempt to incorporate this effect empirically by adding bond-relaxation effects to the model.[8,9] Unfortunately, this adds parameters which cannot be determined from bulk data. Finally, the different atomic sizes of the atoms result in strain energies that are not included in the lattice-gas approach.[10,11]

The statistical mechanics of the lattice-gas models have generally been treated for this problem in two ways. The simplest approach is based on mean-field ideas.[6-8] The entropy of the system is assumed to be just the ideal entropy of mixing. The total energy of the system is approximated by assuming that the number of neighbors of a given type is just the concentration of that species times the number of neighboring lattice sites. For the surface problem, these ideas are generalized by considering each layer separately. The entropy of each layer is given by the mixing entropy for the concentration of that layer, and the energy is computed by taking the number of neighbors in a given layer from the concentration in that layer. The composition of each layer is then determined by requiring the free energy, $E-TS$, to be a minimum. These approximations are reasonable when there is little tendency for the species to cluster or order, but is poor for the cases where these ordering effects are large.

Another approach to the statistical mechanics has been Monte Carlo simulation.[9] Here a series of lattice configurations are generated in accord with the Boltzmann distribution appropriate to the desired temperature. This approach will give an excellent description of the equilibrium associated with the lattice-gas model, but the predictions are still no better than the underlying approximation for the energetics. In general, then, while the lattice-gas techniques usually correctly predict the general trends, they do not constitute a complete treatment of the problem.

Other treatments of the surface segregation problem have concentrated on the strain-energy contributions to segregation.[2,10,11] The strain energy of an impurity or solute atom in the bulk is assumed to be given by the elasticity theory result for the energy of embedding a misfitting sphere into the lattice, and the strain energy on the surface is assumed to be negligible. This implies that for large lattice constant mismatches the dilute species will always segregate to reduce the strain energy. This strain-energy contribution has in some calculations been added to the energetics of a lattice-gas model in order to incorporate the strain contributions. Unfortunately, elasticity theory is not appropriate for quantitatively describing the energies of strains on an atomic scale.[2]

Another approach to the energetics which has been used extensively to describe defects in metals[12] is the pair potential approximation. This approximation has been used to compute the segregation energy to surfaces and defects.[13] The advantage of this approach is that it yields the energy as a function of the atomic separations. The atoms can be allowed to move to their equilibrium positions and the strain energy is included naturally. Monte Carlo simulations of alloy surfaces using Lennard-Jones interactions have been performed by Abraham[2] which allowed for both the variation of the composition at the surface as well as the atomic scale relaxation of the atoms. This work showed that the elasticity theory treatments of the strain energy overestimate the effect especially for the case where the solute has a smaller lattice constant.

While the pair potential model is useful for gaining some qualitative insight into segregation, there are problems with using this approach to describe the energetics of real alloy surfaces. The simplest form of the pair potential approximation writes the total energy as a sum over pairwise interactions. This approach cannot describe the elastic properties of metals since it must yield a vanishing Cauchy discrepancy, $C_{12}-C_{44}$. This problem can be corrected by adding a term to the energy which depends on the average atomic volume. (This contribution is also referred to as the structure-independent energy in the pseudopotential treatments of simple metals.[14]) This term accounts for both the energy of the background electron gas of a metal as well as the average energy of an ion in that electron gas. This volume-dependent term, though, presents a problem for calculations with alloy surfaces. First, it is not clear how to treat this contribution to the energy for atoms in the surface layer since there is no unambiguous way to define an atomic volume. Also, it is not clear that the contributions to the surface energy due to the surface energy of the electron gas and the change in the average interaction of the atom with the electron gas can be reasonably described by simply assigning a different volume to the surface atoms. The need for a volume-dependent term also presents a difficulty for describing alloys. This term must now depend both on the average atomic volume and the overall concentration, but there is no clear way to determine the nature of this dependence.

The embedded-atom method[15-17] (EAM) provides a new framework that avoids many of the problems with the previous approaches. This method has already been applied to pure metals with good results. The applications in the bulk include phonon spectra,[18] structure of liquid metals,[19] defect energies, and fracture properties.[15,16] It has been applied to surfaces and shown to give good results for the surface energy and surface relaxation.[16] It also correctly predicts the (1×2) surface reconstruction of Pt(110) surfaces.[20] The EAM has also been applied to hydrogen interactions with metals. It has predicted the ordered structures and critical temperatures of hydrogen adsorbed on Pd(111),[21] and the influence of hydrogen on fracture.[15] As will be described below, the energy of each atom is determined by the local electron density due to the other atoms of the metal. This density is computed by the superposition of atomic densities. Since this density is well defined both in alloys and at surfaces, there are no ambiguities involved in this method.

Computationally, the EAM energy can be evaluated with about the same amount of work as simple pair potentials. Therefore, it is feasible to perform computer simulations that incorporate both compositional changes and atomic scale relaxation. Therefore the strain effects can be incorporated automatically with the electronic or bonding contributions to the energy. Thus the EAM provides a powerful new technique for determining the composition and structure of alloy surfaces.

The first section of this paper describes the EAM, including the procedures used to determine the empirical functions used in this method. This will be followed by a discussion of the Monte Carlo simulation technique that we will use to determine the statistical mechanics of the system. Next, the predictions of the method for the thermodynamics and short-range order of the bulk Ni-Cu alloys will be presented and compared with experiment. Finally, the results for the surface composition profile of Ni-Cu alloys as a function of bulk composition and crystal face will be presented and compared with experimental results.

II. THEORY

Within density-functional theory, the total electronic energy of an arbitrary arrangement of atoms can be written as a unique functional of the total electron density. The starting point of the embedded-atom method is the observation that the total electron density in the vicinity of a given atom can be thought of as the atomic density of the atom in question plus an electron density from the surrounding atoms. This latter contribution to the total electron density should be a slowly varying function of position, and so it is reasonable to approximate this contribution to the local electron density by a constant. The energy of this atom can then be approximated by the energy associated with the electron density of the atom plus the constant background density. This defines an embedding energy as a function of the background electron density and the atomic species. There is an additional energy contribution from the electrostatic energy due to core-core overlap. These ideas have been developed by Daw and Baskes,[16,17] who show that the total energy can be approximately written

$$E_{\mathrm{tot}}=\sum_i F_i(\rho_{h,i})+\tfrac{1}{2}\sum_{i\neq j}\phi_{ij}(R_{ij}) . \tag{1}$$

In this expression, $\rho_{h,i}$ is the electron density at atom i due to the remaining atoms of the system, $F_i(\rho)$ is the energy to embed atom i into the electron density ρ, and $\phi_{ij}(R_{ij})$ is the core-core pair repulsion between atoms i and j separated by the distance R_{ij}. The electron density is approximated by the superposition of atomic densities,

$$\rho_{h,i}=\sum_{j\,(\neq i)}\rho_j^a(R_{ij})\ , \tag{2}$$

where $\rho_j^a(R)$ is the atomic electron density due to atom j. With this approximation for the electron density, the actual computations using this method do not require significantly more work than the use of pair interaction models. Note that the embedding energy, $F_i(\rho)$, does not depend on the source of the background charge density. Thus the same embedding function would be used to calculate the energy of an atom in an alloy that would be used in the pure material. This makes this method particularly appealing for studies of alloys.

To apply this method, the embedding energies, pair repulsions, and atomic densities must be known. The atomic densities will be taken from Hartree-Fock calculations as discussed below. Approximate values of the embedding energies and pair interactions can be calculated from the formal definitions of these quantities in the density-functional framework as described by Daw.[17] These values, though, only give qualitatively correct predictions of the material properties so it is necessary to determine these functions empirically to obtain an accurate description. The first-principles calculations do give the following important information about the general behavior of these functions. The embedding energy relative to the free-atom energy must go to zero at zero electron density and should have a negative slope and positive curvature for the background electron densities found in metals. The pair interaction term, $\phi(R)$, should be purely repulsive. Further, the pair interaction between atoms of two different species, A and B, is accurately described by the geometric mean of the interactions between the atoms of the same species, i.e.,

$$\phi_{AB}(R)=[\phi_{AA}(R)\phi_{BB}(R)]^{1/2}\ . \tag{3}$$

Daw and Baskes[16] have shown that it is possible to obtain the embedding energy and pair interactions for pure metals empirically. They assume functional forms for $F(\rho)$ and $\phi(R)$ which meet these general conditions and adjust the parameters to fit the known bulk properties of the pure materials. In particular, they fit the sublimation energy, lattice constant, elastic constants, and vacancy formation energy. They also obtain functions for hydrogen and helium. These functions cannot be used to study binary alloys, though. The information used in their empirical fits actually only determines $F(\rho)$ and its low derivatives for electron densities near the average electron density, ρ_{eq}, of the bulk pure materials at equilibrium. While this is sufficient information about $F(\rho)$ for calculations of pure materials, the atoms in an alloy will generally experience rather different electron densities than in the pure bulk material, and so we use values of the embedding function which are not well determined. A main objective of this work is to develop a set of empirical parametrizations which do not have this deficiency and so can reliably describe alloys.

It is possible to obtain information about $F(\rho)$ for densities well away from ρ_{eq} through the equation of state of the expanded or compressed metals since the electron density at each lattice site can be substantially different from ρ_{eq}. Rose *et al.*[22] have shown that the sublimation energy of most metals as a function of lattice constant can be scaled to a simple universal function,

$$E(L)=-E_{\mathrm{sub}}(1+a^*)e^{-a^*}\ . \tag{4}$$

In this expression, L is a length scale of the system which we will take to be the fcc lattice constant, and E_{sub} is the absolute value of the sublimation energy. The quantity a^* is a measure of the deviation from equilibrium,

$$a^*=(L/L_0-1)/[E_{\mathrm{sub}}/(9B\Omega)]^{1/2}\ . \tag{5}$$

Here B is the bulk modulus of the material, L_0 is the equilibrium lattice constant, and Ω is the volume per atom. This expression has been shown to give a good fit to the equation of state of numerous materials over a wide range of both expansion and compression. Further, the only input data needed are the equilibrium density, sublimation energy, and bulk modulus of the material, which are generally readily available.

Note that if the atomic densities, ρ^a, and the pair interaction, $\phi(R)$, are both known, then the embedding energy can be uniquely defined by requiring the total energy of the system given by Eq. (1) to agree with the universal equation of state given by Eq. (4). The problem then is to determine the atomic densities and pair interactions. The atomic density is assumed to be given by the free-atom densities calculated from Hartree-Fock theory by Clementi and Roetti.[23] There is one ambiguity, though, in using these atomic densities for the bulk. While the optimum electronic configuration is known for the free atom, it is not clear that this configuration will be the best representation of the electron density in the solid. For a pure material this is not a serious problem. The main effect of changing the relative number of s and d electrons is to simply change the electron density (for the distances that are actually used in these calculations) by a multiplicative factor. This represents the fact that the d-electron wave functions are quite small at the nearest-neighbor distance. Changing the atomic density by a constant factor, though, does not change the properties computed for a single element, since this change simply results in a rescaling of the argument of the embedding function to yield the same results. For a multicomponent system, though, changing the atomic density used for one of the components will strongly affect the mixing energies of the alloy. Thus it is essential that a consistent choice is made for the electronic configurations assumed for the different metals.

The atomic densities in this work are computed from the Hartree-Fock wave functions by

$$\rho^a(R)=N_s\rho_s(R)+N_d\rho_d(R)\ , \tag{6}$$

where N_s and N_d are the number of outer s and d electrons, and ρ_s and ρ_d are the densities associated with the s and d wave functions. (For Ni the wave functions for the

TABLE I. Parameters used to define the embedding functions and pair potentials. E_{sub} is the sublimation energy, a is the equilibrium fcc lattice constant, B is the bulk modulus, and N_s, Z_0, and α are defined in the text. Energies are expressed in eV, distances in Å, and bulk modulus in eV/Å^3.

	E_{sub}	a	B	Z_0	α	N_s
Ni	4.45	3.52	1.127	10	1.195	2.0
Cu	3.54	3.615	1.383	11	1.513	0.76

$3d^84s^2$ configurations are used, while for Cu the wave functions are for $3d^{10}4s^1$. These are the closest configurations to the values of N_s that will ultimately be used for these calculations.) The total number of s and d electrons, N_s+N_d, is fixed to be 10 for Ni and 11 for Cu. Thus the atomic density of each species depends on the single parameter, N_s. As will be discussed below, this parameter will be determined so as to give the proper heats of solution of the bulk alloys.

The last quantity that is needed is the pair repulsion term. The form of this function has been studied from first principles by Daw.[17] This analysis shows that the function can be reasonably represented by a Yukawa potential form, and that the pair interaction between two different species is accurately approximated by the geometric mean of the pair interaction for the individual species. This leads to writing the pair interaction between atoms of types A and B as

$$\phi_{AB}(R)=Z_A(R)Z_B(R)/R\ , \tag{7}$$

where the effective charge, $Z(R)$, is given by

$$Z(R)=Z_0e^{-\alpha R}\ . \tag{8}$$

The value of Z_0 will be assumed to be given by the number of outer electrons of the atom, i.e., $Z_0=10$ for Ni and $Z_0=11$ for Cu. Thus there is one parameter, α, left to determine the pair interactions.

With the above assumptions, there are two adjustable parameters needed to determine the pair potential, atomic densities, and embedding functions for each material. These have been determined for the elements Ni and Cu to fit the elastic constants of each material as well as the dilute limits of the heats of solution of the binary alloy. Note that due to the definition of the embedding function in terms of the equation of state of the pure materials, the equilibrium lattice constant, sublimation energy, and bulk modulus are guaranteed to be correct for the pure materials. The values of α are essentially determined by the shear properties of the materials, and the ratio of the N_s's is determined by the heats of mixing of the alloys. (The N_s for Ni is arbitrarily chosen to be 2. As discussed above, the N_s for a pure material is arbitrary.) The parameters used to define the functions are given in Table I. These values fit the elastic constants to within 10%, and heats of mixing are fit to within 0.1 eV.

III. MONTE CARLO SIMULATION TECHNIQUE

The equilibrium alloy structure will be computed using Monte Carlo simulation techniques with the energetics described by the EAM. These simulations include two different kinds of variations of the system, the compositional arrangement of the atoms and the spatial relaxation of the atomic positions. The latter feature eliminates one of the major drawbacks of lattice-gas models, namely that lattice strain effects are either ignored or must be added in an *ad hoc* manner. Here the relative atomic positions are allowed to adjust to the composition of their neighbors, and therefore lattice strain energies are included naturally.

The surface simulations are performed for a slab geometry. Periodic boundaries are applied in the directions parallel to the surface. The geometry of the periodic cell depended on the crystal face exposed, but was chosen so that the cell face would be approximately square. The number of surface atoms on each face was 32 for (100) surfaces, 24 for (110) surfaces, and 48 for (111) surfaces. The lattice constants used to determine the periodicities of the calculations were chosen to correspond to the lattice constants of the bulk alloys at the same composition and temperature. The number of atomic layers in each slab also depended on the crystal face, 17 layers for (100) surfaces, 25 layers for (110) surfaces, and 15 layers for (111) surfaces. These values produce slabs which are roughly 30 Å thick. A few simulations with thicker slabs or larger surface areas were performed and the resulting surface compositions were the same as for the above sizes. The simulations performed on bulk alloys used a periodically extended cube of material containing 500 atoms.

The simulations are performed in a grand canonical ensemble where the volume, total number of atoms, and relative chemical potentials of the two species are held fixed. There are two different kinds of basic steps used in the simulations. The first is a small displacement of an atom from its current position. This allows for both the thermal variation in the atomic positions (i.e., vibrational contributions to the free energy), as well as the different equilibrium separations between atoms of different elements. The second basic Monte Carlo step is to change the element of a given atom. This corresponds to the thermodynamic action of taking an atom of the original type out of the solid to a reservoir at infinity and bringing in an atom of the new type from infinity. The inclusion of this type of step has the advantage of greatly increasing the speed with which the simulation converges relative to constant number simulations, since the segregating species does not have to diffuse to the surface. The desired bulk composition is obtained by adjusting the relative chemical potentials.

The simulation proceeds as follows. First an atom is chosen at random and a displacement and/or a new atomic species for that atom is chosen. Next, the total energy of this new arrangement of atoms is computed. The decision to retain this change is made based on ΔP, where

$$P=(N_A!N_B!)^{-1}\exp[-(E-\mu_A N_A-\mu_B N_B)/k_B T] \tag{9}$$

and

$$\Delta P=P_{\text{new}}/P_{\text{old}} \; . \tag{10}$$

Here N_A and N_B refer to the number of atoms of element A and B (Ni and Cu in this case), μ_A and μ_B are the chemical potentials of the two species, E is the total energy, T is the temperature, and k_B is Boltzmann's constant. If $\Delta P>1$, the new configuration is always retained, while if $\Delta P<1$, the new configuration is retained with the probability ΔP. Repeating this procedure a large number of times (several million) results in a set of atomic configurations corresponding to thermal equilibrium. The desired quantities, such as the composition profile, are then obtained by averaging over the resulting configurations. Note that in the case where the number of each species remains the same, this condition reduces to the more common condition that the new configuration is accepted with a probability given by a Boltzmann factor for the change in energy.

IV. BULK ALLOYS

In order to verify that this procedure produces a reasonable description of the bulk alloy, the excess energy and lattice constant of the bulk alloys were computed at $T=800$ K. Also, the short-range ordering of the atomic species was determined. The lattice constants used for these bulk simulations were adjusted so that the average pressure is zero. The pressure can be obtained from the quantity

$$P=nk_BT-(n/6N)\left\langle \sum_{ij,i\neq j}[F_i'(\rho_{h,i})\rho_j^{a\prime}(R_{ij})+F_j'(\rho_{h,i})\rho_i^{a\prime}(R_{ij})+\phi'(R_{ij})]R_{ij}\right\rangle \; . \tag{11}$$

In this expression, the primes refer to derivatives with respect to the argument, n is the total atomic number density, N is the total number of atoms, and the brackets refer to a thermal average. The lattice constants predicted for pure Ni and Cu at 800 K are 3.560 and 3.670 Å, respectively. These values correspond to average values of the linear coefficient of thermal expansion of 14.2 and 18.9 in units of 10^{-6} K^{-1}. The corresponding experimental values[24] for room temperature are 12.7 and 16.7. Thus the EAM provides a good description of the thermal expansion, and so must include reasonable values of the anharmonicity of the interatomic interactions. In Table II the values of the excess enthalpy of Ni-Cu alloys at 800 K for three bulk compositions are compared with experiment.[25] (The excess enthalpy is the difference between the enthalpy of the alloy and the linear interpolation of the enthalpy between that of the two pure materials.) The agreement between the two is good as expected since the dilute limits of these values are used in the fitting process. Note that the EAM produces the same asymmetry in the excess enthalpy as is found in experiment. The deviations of the lattice constant from Vegard's law are also compared with experiment[26] in Table II. (Vegard's law states that the lattice constant varies linearly with composition.)

TABLE II. The excess enthalpy (ΔH) and deviation of the lattice constant from Vegard's law (Δa) as a function of composition, X_{Cu}, for bulk Ni-Cu alloys. The experimental enthalpies are from Ref. 25 and the experimental lattice constants are from Ref. 26.

X_{Cu} (at. %)	ΔH_{theor} (eV)	ΔH_{expt} (eV)	Δa_{theor} (Å)	Δa_{expt} (Å)
30.4	0.019	0.019	0.020	-0.004
50.6	0.014	0.018	0.027	-0.005
74.2	0.008	0.009	0.025	-0.003

Unfortunately, the agreement here between theory and experiment is poor. The EAM predicts that the alloys would have a slightly larger lattice constant then Vegard's law, while experiment predicts an even smaller deviation in the opposite direction. However, this represents the deviation from the main trend, and so does not represent a serious disagreement between theory and experiment, i.e., the lattice constants are correctly predicted to within <0.03 Å.

In order to test the predictions of the theory for short-range compositional order, the Warren-Cowley short-range order parameters,[27] α_i, have been determined. This quantity measures the probability of finding neighboring atoms with either the same or opposite type. It is defined by

$$\alpha_i=1-(p_i^{AB}/X_B) \; , \tag{12}$$

where the subscript i refers to the ith shell of neighbors, p_i^{AB} is the probability that a specific atom in the ith neighbor shell around an atom of type A will be of type B, and X_B is the concentration of species B. A positive value of α indicates a tendency for atoms of the same type to cluster. The values of α determined at $T=800$ K for the first five neighbor shells are presented in Table III. The experimental diffuse neutron-scattering results for Ni-Cu alloys have been reviewed by Vrijen and Radelaar.[28] There is a significant amount of spread between the different experimental values, but α_1 is generally in the range 0.08 to 0.14 for the compositions and temperature shown here. The values past first neighbors are smaller for both experiment and theory. Thus the short-range compositional order predicted by the EAM appears to be reasonable.

V. Ni-Cu ALLOY SURFACES

From the macroscopic thermodynamic point of view, surface segregation phenomena are driven by the differ-

TABLE III. Warren-Cowley short-range-order coefficient, α_i, for the bulk Ni-Cu alloys computed at $T=800$ K.

X_{Cu} (at. %)	α_1	α_2	α_3	α_4	α_5
28.4	0.149	0.033	0.013	0.003	0.000
50.8	0.137	0.001	−0.015	−0.018	−0.017
72.2	0.085	−0.031	−0.027	−0.019	−0.014

ences in surface energy for various surface compositions. Therefore, the surface energies of the two pure materials have been calculated using the EAM to verify that the method gives reasonable values. The surface energy is computed by minimizing the energy of a slab of atoms with respect to all atomic positions to incorporate surface relaxation effects. The surface energy is then the difference between the energy of the slab and that of an equal number of atoms in the bulk. The resulting values are 1780, 1940, and 1650 ergs/cm^2 for the (100), (110), and (111) faces of Ni. The corresponding numbers for Cu are 1210, 1320, and 1100 ergs/cm^2. Tyson and Miller[29] quote average surface energies extrapolated to $T=0$ K of 2270 for Ni and 1790 ergs/cm^2 for Cu. This agreement between theory and experiment is reasonable since there is a wide spread in the experimental values for the solid surface energies and the experimental values are averages over various surface orientations. The theoretical values are for ideal low index faces which one would expect to have a below average surface energy. More important for segregation phenomena, the theory predicts the correct relative size of the surface energies for the two materials.

The heat of segregation in the dilute limit has also been determined. The heat of segregation is usually defined as the difference in energy for placing an impurity or solute atom at the surface of an otherwise pure material relative to placing the atom in the bulk. This quantity is generalized here to a segregation energy for each atomic plane. This energy is determined by computing the total energy of slabs containing a single impurity in different atomic planes near the surface relative to the energy of that impurity in the bulk. The results are presented in Table IV, for the three low index faces. As expected, the segregation energy for Cu on Ni surfaces is negative and that for Ni in the first layer of Cu is positive. This is in accord with the known segregation of Cu to the surface of these alloys.[3] The segregation energy for Cu in the first layer of the Ni(100) surface has been determined experimentally by Egelhoff[30,31] using x-ray photoemission spectroscopy. The approach is based on the equivalent-core approximation which states that an atom of nuclear charge Z is equivalent to an atom of charge $Z+1$ after an inner shell electron is ionized. The heat of segregation of element $(Z+1)$ in element Z can then be identified with the difference between the core-level binding shifts of bulk and surface atoms. His value of -0.43 ± 0.04 eV for this heat of segregation is in excellent agreement with the theoretical value determined here. This further supports the validity of the energetics described by the EAM.

The surprising feature of the results in Table IV are the heats of segregation to the planes just below the surface. Here the energies show that Ni is attracted to the second or third atomic plane, or equivalently that Cu is repelled from these planes. This oscillation of the heat of segregation suggests that the composition profile should not be monotonic. This agrees with the experimental results of Ng *et al.*[32] using field ion microscopy. They observed a depletion of Cu from the near-surface atomic planes for a Ni-Cu (5 at. %) sample at $T=800$ K.

The above heats of segregation are for the extreme dilute limits. Since these energies are fairly large, one expects that the surface layer will be strongly enriched in Cu for all bulk compositions. This change in local composition will affect the energetics of the atoms near the surface. Therefore, the above heats of segregation cannot be used to estimate surface compositions. It is also necessary to incorporate the thermal effects. As discussed above, these factors will be incorporated by performing Monte Carlo simulations. All of the simulations have been performed at a temperature of 800 K. This temperature is in the range of the temperatures for the various experimental studies of this system. Simulations have been performed for the three low index faces for a variety of bulk compositions spanning the entire concentration range.

TABLE IV. The segregation energies Q_i, expressed in eV, of a single Cu (Ni) impurity to the ith surface layer in a Ni (Cu) slab at $T=0$ K. The segregation energy is the total energy of the slab with the impurity in the ith surface layer relative to the energy of the impurity in the bulk.

	Q_1	Q_2	Q_3	Q_4
Cu in Ni(100)	−0.426	0.045	0.002	
Ni(110)	−0.538	−0.029	0.039	0.002
Ni(111)	−0.304	0.029	0.000	
Ni in Cu(100)	0.233	−0.147	−0.002	
Cu(110)	0.349	−0.115	−0.092	−0.005
Cu(111)	0.160	−0.090	0.002	

TABLE V. The calculated composition profile in at. % Cu for Ni-Cu alloys at $T=800$ K. The subscripts refer to the atomic layers.

Face	X_{bulk}	X_1	X_2	X_3	X_4	X_5
(111)	4.8	89.4	3.0	4.0	5.0	4.8
	29.2	95.0	11.0	19.1	27.1	29.0
	55.2	96.2	21.3	43.2	56.9	57.0
	71.9	97.5	39.0	70.2	76.8	71.3
	93.3	99.1	79.3	93.8	93.6	92.8
(100)	25.0	97.5	11.7	11.6	18.6	23.5
	57.0	98.1	22.7	36.6	57.7	60.3
	73.9	98.7	38.6	60.9	78.1	75.8
(110)	29.1	99.1	36.8	14.1	19.8	27.0
	55.1	99.4	43.9	25.4	40.3	54.0
	72.0	99.7	55.8	44.3	64.8	76.3

The layer by layer compositions computed from the simulations are presented in Table V, and the concentration of the first three layers of the (111) surfaces are plotted as a function of bulk concentration in Fig. 1. In addition, the atomic number density of each component is plotted as a function of depth into the slab in Fig. 2 for the (111) face of a 71 at. % Ni alloy. The trends suggested by the segregation energies in the dilute limit are retained in these results. The first layer is almost pure Cu for all the compositions studied here. Further, there is a noticeable enrichment of Ni in the near surface atomic layers. The results for the (100) and (111) faces are very similar though the segregation of Cu is somewhat stronger to the (100) surface. This agrees with the expectations from simple bond-breaking arguments. On the other hand, the enrichment of Ni in the second layer is somewhat less pronounced for the (100) face than for the (111) face. The strongest enrichment of Cu is found in the top surface layer of the (110) face. For this face, the composition profile is still nonmonotonic, but the maximum Ni concentration is found in the third atomic layer.

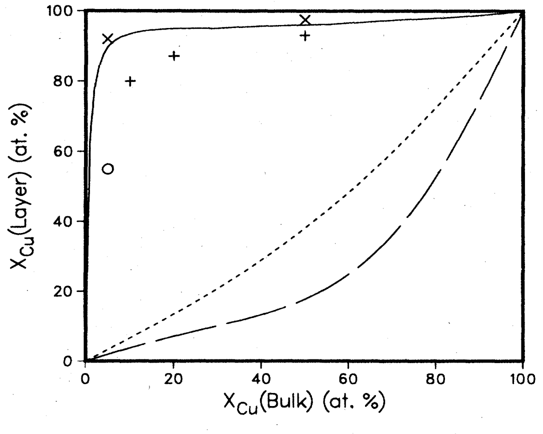

FIG. 1. Calculated Cu layer concentrations as a function of bulk composition at $T=800$ K for (111) face of Ni-Cu alloys. The solid curve is the top layer, the long-dashed curve is the second layer, and the short-dashed curve is the third layer. The points are the experimental values for the top layer from Ref. 32 (○), Ref. 33 (×), and Ref. 38 (+).

The atomic positions of the surface atoms are similar to those for a pure metal surface. This is not surprising since the lattice constants of Ni and Cu are not very different, 3.52 and 3.62 Å, respectively. The atomic densities plotted in Fig. 2 do show an interesting feature which is found at all compositions. The average position of the Cu atoms is slightly above that of the Ni atoms. This is reasonable since Cu has the larger lattice constant. This difference is fairly small, 0.1—0.2 Å, and depends on temperature. The difference in height found at $T=0$ K from energy minimization of a few characteristic structures showed smaller differences in the height of the two species. Thus this difference is in part due to the differences in the vibrations of the two species.

There have been several experimental studies of the surface composition of Ni-Cu alloys using Auger-electron spectroscopy (AES),[33–37] low-energy ion scattering[38] (LEIS), field ion microscopy[32] (FIM), and sputtering.[39] Although early AES studies did not find any segregation, all the recent work indicates that there is substantial segregation of Cu to the surface in agreement with the present calculations. Most of these studies used polycrystalline samples, so detailed comparisons with the above re-

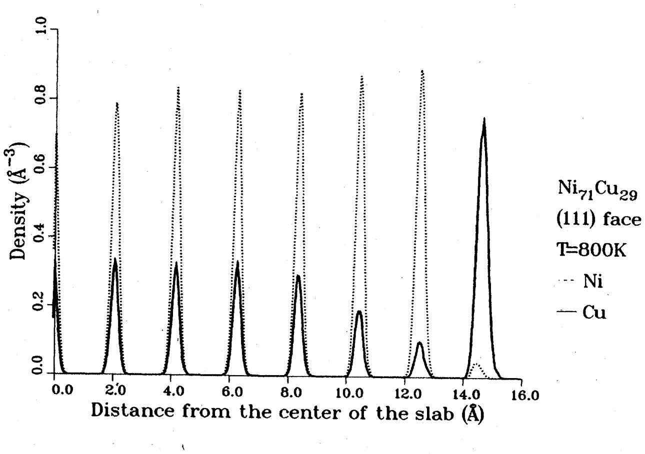

FIG. 2. Calculated atomic number density of Cu (solid line) and Ni (dotted line) averaged over planes parallel to the (111) surface as a function of the distance from the center of the computational slab. These results are for a bulk Cu concentration of 29 at. % at $T=800$ K.

sults is not possible. However, it is interesting to note that the early segregation studies which did not show segregation used AES with high-energy transitions where the escape depths of the emitted electrons are several atomic layers. Thus the compositions that were produced represent a weighted average over the first few atomic layers. The composition oscillations that are found here would then explain why the average composition near the surface found in the early experiments was close to the bulk values. The more recent AES experiments have used lower-energy transitions, where the emitted electrons have much shorter escape depths and so are more sensitive to the surface layer. Another potential experimental problem is the effect of impurities. There is evidence[40,41] that the presence of S, CO, or H on the surface will decrease the Cu segregation. This reflects the stronger bonding of the Ni to these impurities on the surface. Thus only experiments with high surface cleanliness will yield reliable surface compositions.

There have been three studies appropriate to single-crystal (111) faces.[32,33,38] The results of these experiments for the top-layer composition are compared with the theoretical predictions in Fig. 1. The agreement is good. The AES and x-ray photoemission results of Webber *et al.*[33] are for a temperature of 880 K. They used various electron energies to determine the ratio of Ni to Cu signals for different escape depths. A total composition profile could then, in principle, be determined by using the different attenuations appropriate for the various transitions. The top-layer composition that they determined at bulk concentrations of 5 at. % and 50 at. % Cu are 85—100 at. % Cu and 95—100 at. % Cu, respectively, in good agreement with our results. Their results for the deeper layers are less clear since a range of profiles agree with their experimental measurements. In general, the Cu enrichment is restricted to a small layer near the surface, and they saw some indications of oscillations in the profile out to around 12 Å. These conclusions are also in accord with our results.

The FIM result of Ng *et al.*[32] are obtained by mass analyzing the atoms produced by field evaporation. By analyzing only the atoms coming from the edge of a step, a layer profile is obtained. The results show that the Cu concentration is depleted in the second and third layers below the surface. This depletion of Cu near the surface is in accord with our calculations. There is a significant difference in the compositions determined for the first layer. This could be due to the geometry of the tip. The experiment probes a (111) facet which only approximates an ideal planar geometry. Since the bulk composition is in a region where the surface composition is varying rapidly, this finite geometry may have a significant effect.

VI. SUMMARY

The EAM has been applied to the computation of the surface composition of Ni-Cu alloys. The segregation energy in the dilute limit agrees with the experimental values, and the composition profiles at finite temperature and for the full range of compositions are in accord with the experimental information. The method also provides a good description of the energetics and short-range order of the bulk alloys. Thus the EAM in conjunction with computer simulations provides a reasonable description of the Ni-Cu alloy system.

The advantage of this approach is that it is capable of describing a wide range of alloy systems. The use of a technique that allows for the spatial relaxation of the atoms means that the method is not restricted to alloy systems where the lattice mismatch is small. The use of Monte Carlo simulations allows reliable predictions to be made for systems that show significant amounts of ordering or clustering. The method is also capable of determining the ordering behavior of the surface. Finally, the EAM only requires *bulk* data to describe the surfaces. Thus there is not a need for extensive surface information about a system before it can be studied. Therefore the EAM provides a powerful new technique for describing the properties of alloy surfaces.

ACKNOWLEDGMENTS

This work was supported by the U. S. Department of Energy (Office of Basic Energy Sciences).

---

[1] S. H. Overbury, P. A. Bertrand, and G. A. Somorjai, Chem. Rev. **75**, 547 (1975).

[2] F. F. Abraham and C. R. Brundle, J. Vac. Sci. Technol. **18**, 506 (1981).

[3] M. J. Kelly and V. Ponec, Progr. Surf. Sci. **11**, 139 (1981).

[4] A. R. Miedema, Z. Metallkd. **69**, 455 (1978).

[5] J. C. Hamilton, Phys. Rev. Lett. **42**, 989 (1979).

[6] F. L. Williams and D. Nason, Surf. Sci. **45**, 377 (1974).

[7] V. S. Sundaram and P. Wynblatt, Surf. Sci. **52**, 569 (1975).

[8] V. Kumar, Phys. Rev. B **23**, 3756 (1981).

[9] T. S. King and R. G. Donnelly, Surf. Sci. **141**, 417 (1984).

[10] P. Wynblatt and R. C. Ku, Surf. Sci. **65**, 511 (1977).

[11] Y. W. Lee and H. I. Aaronson, Surf. Sci. **95**, 227 (1980).

[12] M. I. Baskes and C. F. Melius, Phys. Rev. B **20**, 3197 (1979).

[13] R. Wynblatt and D. A. Steigerwald, Surf. Sci. **150**, 289 (1985).

[14] N. W. Ashcroft and D. Stroud, in *Solid State Physics*, edited by F. Seitz, D. Turnbull, and H. Ehrenreich (Academic, New York, 1978), Vol. 33, p. 1.

[15] M. S. Daw and M. I. Baskes, Phys. Rev. Lett. **50**, 1285 (1983).

[16] M. S. Daw and M. I. Baskes, Phys. Rev. B **29**, 6443 (1984).

[17] M. S. Daw (unpublished).

[18] M. S. Daw and R. L. Hatcher, Solid State Commun. (to be published).

[19] S. M. Foiles, Phys. Rev. B **32**, 3409 (1985).

[20] M. S. Daw, Surf. Sci. Lett. (to be published).

[21] T. E. Felter, S. M. Foiles, M. S. Daw, and R. H. Stulen, Surf. Sci. Lett. (to be published).

[22] J. H. Rose, J. R. Smith, F. Guinea, and J. Ferrante, Phys. Rev. B **29**, 2963 (1984).

[23] E. Clementi and C. Roetti, At. Data Nucl. Data Tables **14**,

177 (1974).

[24] K. A. Gschneidner, Jr., in *Solid State Physics,* edited by F. Seitz, D. Turnbull, H. Ehrenreich (Academic, New York, 1964), Vol. 16, p. 276.

[25] R. Hultgren, P. D. Desai, D. T. Hawkins, M. Gleiser, and K. K. Kelly, *Selected Values of the Thermodynamic Properties of Binary Alloys* (American Society for Metals, Cleveland, 1973).

[26] B. R. Coles, J. Inst. Met. **84**, 346 (1955).

[27] J. M. Cowley, Phys. Rev. **77**, 669 (1950).

[28] J. Vrijen and S. Radelaar, Phys. Rev. B **17**, 409 (1978).

[29] W. R. Tyson and W. A. Miller, Surf. Sci. **62**, 267 (1977).

[30] W. F. Egelhoff, Jr., Phys. Rev. Lett. **50**, 587 (1983).

[31] W. F. Egelhoff, Jr., Phys. Rev. B **30**, 1052 (1984).

[32] Y. S. Ng, T. T. Tsong, and S. B. McLane, Jr., Phys. Rev. Lett. **42**, 588 (1979).

[33] P. R. Webber, C. E. Rojas, P. J. Dobson, and D. Chadwick, Surf. Sci. **105**, 20 (1981).

[34] K. Wandelt and C. R. Brundle, Phys. Rev. Lett. **46**, 1529 (1981).

[35] F. J. Kuijers and V. Ponec, Surf. Sci. **68**, 294 (1977).

[36] C. R. Helms and K. Y. Yu, J. Vac. Sci. Tech. **12**, 276 (1975).

[37] K. Watanabe, M. Hashiba, and T. Yamashina, Surf. Sci. **61**, 483 (1976).

[38] H. H. Brongersma, M. J. Sparnay, and T. M. Buck, Surf. Sci. **71**, 657 (1978).

[39] D. G. Swartfager, S. B. Ziemecki, and M. J. Kelly, J. Vac. Sci. Technol. **19**, 185 (1981).

[40] S. Ichimura, M. Shikuta, and R. Shimizu, Surf. Sci. **108**, L393 (1981).

[41] D. Tomanek, S. Mukherjee, V. Kumar, and K. H. Bennemann, Surf. Sci. **114**, 11 (1982).